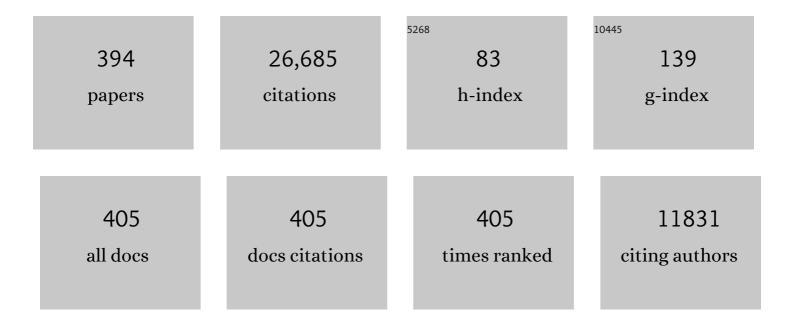
Wolfgang Lubitz

List of Publications by Year in descending order

Source: https://exaly.com/author-pdf/985634/publications.pdf Version: 2024-02-01



#	Article	IF	CITATIONS
1	Hydrogenases. Chemical Reviews, 2014, 114, 4081-4148.	47.7	1,653
2	Hydrogen:  An Overview. Chemical Reviews, 2007, 107, 3900-3903.	47.7	628
3	Biomimetic assembly and activation of [FeFe]-hydrogenases. Nature, 2013, 499, 66-69.	27.8	597
4	[NiFe] and [FeFe] Hydrogenases Studied by Advanced Magnetic Resonance Techniques. Chemical Reviews, 2007, 107, 4331-4365.	47.7	458
5	Biological Water Oxidation. Accounts of Chemical Research, 2013, 46, 1588-1596.	15.6	453
6	Electronic structure of the oxygen-evolving complex in photosystem II prior to O-O bond formation. Science, 2014, 345, 804-808.	12.6	432
7	Solar water-splitting into H2 and O2: design principles of photosystem II and hydrogenases. Energy and Environmental Science, 2008, 1, 15.	30.8	388
8	14N HYSCORE investigation of the H-cluster of [FeFe] hydrogenase: evidence for a nitrogen in the dithiol bridge. Physical Chemistry Chemical Physics, 2009, 11, 6592.	2.8	354
9	Two Interconvertible Structures that Explain the Spectroscopic Properties of the Oxygenâ€Evolving Complex of Photosystemâ€II in the S ₂ State. Angewandte Chemie - International Edition, 2012, 51, 9935-9940.	13.8	342
10	Spontaneous activation of [FeFe]-hydrogenases by an inorganic [2Fe] active site mimic. Nature Chemical Biology, 2013, 9, 607-609.	8.0	316
11	Metal oxidation states in biological water splitting. Chemical Science, 2015, 6, 1676-1695.	7.4	275
12	Theoretical Evaluation of Structural Models of the S ₂ State in the Oxygen Evolving Complex of Photosystem II: Protonation States and Magnetic Interactions. Journal of the American Chemical Society, 2011, 133, 19743-19757.	13.7	271
13	Hydrogens detected by subatomic resolution protein crystallography in a [NiFe] hydrogenase. Nature, 2015, 520, 571-574.	27.8	267
14	Energy and environment policy case for a global project on artificial photosynthesis. Energy and Environmental Science, 2013, 6, 695.	30.8	264
15	Direct Detection of a Hydrogen Ligand in the [NiFe] Center of the Regulatory H2-Sensing Hydrogenase fromRalstoniaeutrophain Its Reduced State by HYSCORE and ENDOR Spectroscopy. Journal of the American Chemical Society, 2003, 125, 13075-13083.	13.7	259
16	Detection of the Water-Binding Sites of the Oxygen-Evolving Complex of Photosystem II Using W-Band ¹⁷ O Electron–Electron Double Resonance-Detected NMR Spectroscopy. Journal of the American Chemical Society, 2012, 134, 16619-16634.	13.7	248
17	Electronic Structure of the Mn ₄ O <i>_x</i> Ca Cluster in the S ₀ and S ₂ States of the Oxygen-Evolving Complex of Photosystem II Based on Pulse ⁵⁵ Mn-ENDOR and EPR Spectroscopy. Journal of the American Chemical Society, 2007, 129, 13421-13435.	13.7	230
18	P700: the primary electron donor of photosystem I. Biochimica Et Biophysica Acta - Bioenergetics, 2001, 1507, 61-79.	1.0	225

#	Article	IF	CITATIONS
19	3-mm High-field EPR on semiquinone radical anions Q.cntdot related to photosynthesis and on the primary donor P.cntdot.+ and acceptor QA.cntdot in reaction centers of Rhodobacter sphaeroides R-26. The Journal of Physical Chemistry, 1993, 97, 7639-7647.	2.9	220
20	[NiFe] hydrogenases: A common active site for hydrogen metabolism under diverse conditions. Biochimica Et Biophysica Acta - Bioenergetics, 2013, 1827, 986-1002.	1.0	219
21	Effect of Ca ²⁺ /Sr ²⁺ Substitution on the Electronic Structure of the Oxygen-Evolving Complex of Photosystem II: A Combined Multifrequency EPR, ⁵⁵ Mn-ENDOR, and DFT Study of the S ₂ State. Journal of the American Chemical Society, 2011, 133, 3635-3648.	13.7	211
22	A redox hydrogel protects hydrogenase from high-potential deactivation and oxygen damage. Nature Chemistry, 2014, 6, 822-827.	13.6	209
23	Single Crystal EPR Studies of the Reduced Active Site of [NiFe] Hydrogenase fromDesulfovibrio vulgarisMiyazaki F. Journal of the American Chemical Society, 2003, 125, 83-93.	13.7	196
24	Calculating the Electron Paramagnetic Resonance Parameters of Exchange Coupled Transition Metal Complexes Using Broken Symmetry Density Functional Theory:Â Application to a MnIII/MnIVModel Compound. Journal of the American Chemical Society, 2004, 126, 2613-2622.	13.7	194
25	Identification and Characterization of the "Superâ€Reduced―State of the Hâ€Cluster in [FeFe] Hydrogenase: A New Building Block for the Catalytic Cycle?. Angewandte Chemie - International Edition, 2012, 51, 11458-11462.	13.8	184
26	Ultrafast Transient Absorption Studies on Photosystem I Reaction Centers from Chlamydomonas reinhardtii. 1. A New Interpretation of the Energy Trapping and Early Electron Transfer Steps in Photosystem I. Biophysical Journal, 2003, 85, 3899-3922.	0.5	180
27	[NiFe] hydrogenases: structural and spectroscopic studies of the reaction mechanism. Dalton Transactions, 2009, , 7577.	3.3	179
28	55Mn Pulse ENDOR at 34 GHz of the S0and S2States of the Oxygen-Evolving Complex in Photosystem II. Journal of the American Chemical Society, 2005, 127, 2392-2393.	13.7	174
29	Structural adaptations of photosynthetic complex I enable ferredoxin-dependent electron transfer. Science, 2019, 363, 257-260.	12.6	162
30	Radicals, Radical Pairs and Triplet States in Photosynthesis. Accounts of Chemical Research, 2002, 35, 313-320.	15.6	161
31	The electronic structure of the primary donor cation radical in Rhodobacter sphaeroides R-26: ENDOR and TRIPLE resonance studies in single crystals of reaction centers. Biochimica Et Biophysica Acta - Bioenergetics, 1993, 1183, 139-160.	1.0	159
32	A five-coordinate Mn(<scp>iv</scp>) intermediate in biological water oxidation: spectroscopic signature and a pivot mechanism for water binding. Chemical Science, 2016, 7, 72-84.	7.4	158
33	The Electronic Structure of the H-Cluster in the [FeFe]-Hydrogenase from <i>Desulfovibrio desulfuricans</i> : A Q-band ⁵⁷ Fe-ENDOR and HYSCORE Study. Journal of the American Chemical Society, 2007, 129, 11447-11458.	13.7	157
34	Direct Observation of an Iron-Bound Terminal Hydride in [FeFe]-Hydrogenase by Nuclear Resonance Vibrational Spectroscopy. Journal of the American Chemical Society, 2017, 139, 4306-4309.	13.7	155
35	Characterization of a unique [FeS] cluster in the electron transfer chain of the oxygen tolerant [NiFe] hydrogenase from <i>Aquifex aeolicus</i> . Proceedings of the National Academy of Sciences of the United States of America, 2011, 108, 6097-6102.	7.1	154
36	Water oxidation in photosystem II. Photosynthesis Research, 2019, 142, 105-125.	2.9	149

3

#	Article	IF	CITATIONS
37	Ammonia binding to the oxygen-evolving complex of photosystem II identifies the solvent-exchangeable oxygen bridge (μ-oxo) of the manganese tetramer. Proceedings of the National Academy of Sciences of the United States of America, 2013, 110, 15561-15566.	7.1	148
38	Ultrafast Transient Absorption Studies on Photosystem I Reaction Centers from Chlamydomonas reinhardtii. 2: Mutations near the P700 Reaction Center Chlorophylls Provide New Insight into the Nature of the Primary Electron Donor. Biophysical Journal, 2006, 90, 552-565.	0.5	146
39	Membrane-Bound Hydrogenase I from the Hyperthermophilic Bacterium <i>Aquifex aeolicus</i> : Enzyme Activation, Redox Intermediates and Oxygen Tolerance. Journal of the American Chemical Society, 2010, 132, 6991-7004.	13.7	145
40	The primary and secondary acceptors in bacterial photosynthesis III. Characterization of the quinone radicals Q A â^' â‹ and Q B â^' â‹ by EPR and ENDOR. Applied Magnetic Resonance, 1999, 17, 1-48.	1.2	142
41	Proton Coupled Electronic Rearrangement within the H-Cluster as an Essential Step in the Catalytic Cycle of [FeFe] Hydrogenases. Journal of the American Chemical Society, 2017, 139, 1440-1443.	13.7	142
42	Spectroelectrochemical Characterization of the Active Site of the [FeFe] Hydrogenase HydA1 from <i>Chlamydomonas reinhardtii</i> . Biochemistry, 2009, 48, 7780-7786.	2.5	133
43	A Model of the [FeFe] Hydrogenase Active Site with a Biologically Relevant Azadithiolate Bridge: A Spectroscopic and Theoretical Investigation. Angewandte Chemie - International Edition, 2011, 50, 1439-1443.	13.8	130
44	Importance of the Protein Framework for Catalytic Activity of [FeFe]-Hydrogenases. Journal of Biological Chemistry, 2012, 287, 1489-1499.	3.4	129
45	A New Quantum Chemical Approach to the Magnetic Properties of Oligonuclear Transitionâ€Metal Complexes: Application to a Model for the Tetranuclear Manganese Cluster of Photosystemâ€II. Chemistry - A European Journal, 2009, 15, 5108-5123.	3.3	123
46	Current Understanding of the Mechanism of Water Oxidation in Photosystem II and Its Relation to XFEL Data. Annual Review of Biochemistry, 2020, 89, 795-820.	11.1	123
47	The Crystal Structure of the [NiFe] Hydrogenase from the Photosynthetic Bacterium Allochromatium vinosum: Characterization of the Oxidized Enzyme (Ni-A State). Journal of Molecular Biology, 2010, 402, 428-444.	4.2	122
48	A Systematic Density Functional Study of the Zero-Field Splitting in Mn(II) Coordination Compounds. Inorganic Chemistry, 2008, 47, 134-142.	4.0	121
49	Structure of the oxygen-evolving complex of photosystem II: information on the S2 state through quantum chemical calculation of its magnetic properties. Physical Chemistry Chemical Physics, 2009, 11, 6788.	2.8	121
50	New Redox States Observed in [FeFe] Hydrogenases Reveal Redox Coupling Within the H-Cluster. Journal of the American Chemical Society, 2014, 136, 11339-11346.	13.7	121
51	Electronic Structure of Antiferromagnetically Coupled Dinuclear Manganese (MnIIIMnIV) Complexes Studied by Magnetic Resonance Techniques. Journal of the American Chemical Society, 1998, 120, 13104-13120.	13.7	120
52	Time-Resolved X-, K-, and W-Band EPR of the Radical Pair State of Photosystem I in Comparison with in Bacterial Reaction Centers. Journal of Physical Chemistry B, 1997, 101, 1437-1443.	2.6	118
53	Hydrogen Bond Geometries from Electron Paramagnetic Resonance and Electronâ ``Nuclear Double Resonance Parameters:  Density Functional Study of Quinone Radical Anionâ ``Solvent Interactions. Journal of the American Chemical Society, 2004, 126, 3280-3290.	13.7	118
54	ENDOR Studies of the Primary Donor Cation Radical in Mutant Reaction Centers of Rhodobacter sphaeroides with Altered Hydrogen-Bond Interactions. Biochemistry, 1995, 34, 8130-8143.	2.5	114

#	Article	IF	CITATIONS
55	Hybrid [FeFe]-Hydrogenases with Modified Active Sites Show Remarkable Residual Enzymatic Activity. Biochemistry, 2015, 54, 1474-1483.	2.5	113
56	Electronic structure of Q-A in reaction centers from Rhodobacter sphaeroides. I. Electron paramagnetic resonance in single crystals. Biophysical Journal, 1995, 69, 311-322.	0.5	112
57	Time-resolved W-band (95 GHz) EPR spectroscopy of Zn-substituted reaction centers of Rhodobacter sphaeroides R-26. Chemical Physics, 1995, 194, 361-370.	1.9	110
58	EPR Study of the Molecular and Electronic Structure of the Semiquinone Biradical QA-•QB-•in Photosynthetic Reaction Centers fromRhodobactersphaeroides. Journal of the American Chemical Society, 2000, 122, 7327-7341.	13.7	110
59	An orientation-selected ENDOR and HYSCORE study of the Ni-C active state of Desulfovibrio vulgaris Miyazaki F hydrogenase. Journal of Biological Inorganic Chemistry, 2005, 10, 51-62.	2.6	110
60	Determination of the g tensor of the primary donor cation radical in single crystals of Rhodobacter sphaeroides R-26 reaction centers by 3-mm high-field EPR. The Journal of Physical Chemistry, 1993, 97, 2015-2020.	2.9	109
61	Relativistic DFT Calculations of the Paramagnetic Intermediates of [NiFe] Hydrogenase. Implications for the Enzymatic Mechanism. Journal of the American Chemical Society, 2001, 123, 5839-5840.	13.7	109
62	Orientation and Electronic Structure of the Primary Donor Radical Cation in Photosystem I:  A Single Crystals EPR and ENDOR Study. Journal of Physical Chemistry B, 2001, 105, 1225-1239.	2.6	106
63	Isolation and first EPR characterization of the [FeFe]-hydrogenases from green algae. Biochimica Et Biophysica Acta - Bioenergetics, 2008, 1777, 410-416.	1.0	104
64	Intermediates in the Catalytic Cycle of [NiFe] Hydrogenase: Functional Spectroscopy of the Active Site. ChemPhysChem, 2010, 11, 1127-1140.	2.1	104
65	A single-crystal ENDOR and density functional theory study of the oxidized states of the [NiFe] hydrogenase from Desulfovibrio vulgaris Miyazaki F. Journal of Biological Inorganic Chemistry, 2006, 11, 41-51.	2.6	103
66	Electronic Structure of Neutral Tryptophan Radicals in Ribonucleotide Reductase Studied by EPR and ENDOR Spectroscopy. Journal of the American Chemical Society, 1996, 118, 8111-8120.	13.7	101
67	A Functional [NiFe]-Hydrogenase Model Compound That Undergoes Biologically Relevant Reversible Thiolate Protonation. Journal of the American Chemical Society, 2012, 134, 20745-20755.	13.7	101
68	In Situ EPR Study of the Redox Properties of CuO–CeO ₂ Catalysts for Preferential CO Oxidation (PROX). ACS Catalysis, 2016, 6, 3520-3530.	11.2	97
69	Recent developments in biological water oxidation. Current Opinion in Chemical Biology, 2016, 31, 113-119.	6.1	97
70	Hydride bridge in [NiFe]-hydrogenase observed by nuclear resonance vibrational spectroscopy. Nature Communications, 2015, 6, 7890.	12.8	96
71	Influence of the Axial Ligands on the Spectral Properties of P700 of Photosystem I:  A Study of Site-Directed Mutants. Biochemistry, 2000, 39, 13012-13025.	2.5	95
72	A Metal–Metal Bond in the Light-Induced State of [NiFe] Hydrogenases with Relevance to Hydrogen Evolution. Journal of the American Chemical Society, 2013, 135, 3915-3925.	13.7	95

#	Article	IF	CITATIONS
73	The [FeFe]â€hydrogenase maturase HydF from <i>Clostridium acetobutylicum</i> contains a CO and CN ^{â^'} ligated iron cofactor. FEBS Letters, 2010, 584, 638-642.	2.8	94
74	A Tyrosylâ^'Dimanganese Coupled Spin System is the Native Metalloradical Cofactor of the R2F Subunit of the Ribonucleotide Reductase of Corynebacterium ammoniagenes. Journal of the American Chemical Society, 2010, 132, 11197-11213.	13.7	93
75	ENDOR Spectroscopy— A Promising Technique for Investigating the Structure of Organic Radicals. Angewandte Chemie International Edition in English, 1984, 23, 173-194.	4.4	92
76	Structure and function of [NiFe] hydrogenases. Journal of Biochemistry, 2016, 160, 251-258.	1.7	92
77	Comparative Study of Reaction Centers from Photosynthetic Purple Bacteria: Electron Paramagnetic Resonance and Electron Nuclear Double Resonance Spectroscopy. Biochemistry, 1994, 33, 12077-12084.	2.5	90
78	Orientation-Resolving Pulsed Electron Dipolar High-Field EPR Spectroscopy on Disordered Solids:Â I. Structure of Spin-Correlated Radical Pairs in Bacterial Photosynthetic Reaction Centers. Journal of Physical Chemistry B, 2007, 111, 6245-6262.	2.6	90
79	Hydrogen Bonding to P700:  Site-Directed Mutagenesis of Threonine A739 of Photosystem I in Chlamydomonas reinhardtii,. Biochemistry, 2002, 41, 8557-8569.	2.5	88
80	Relativistic DFT calculation of the reaction cycle intermediates of [NiFe] hydrogenase: a contribution to understanding the enzymatic mechanism. Journal of Inorganic Biochemistry, 2004, 98, 862-877.	3.5	87
81	A Redox Hydrogel Protects the O ₂ â€Sensitive [FeFe]â€Hydrogenase from <i>Chlamydomonas reinhardtii</i> from Oxidative Damage. Angewandte Chemie - International Edition, 2015, 54, 12329-12333.	13.8	87
82	Spin State as a Marker for the Structural Evolution of Nature's Water-Splitting Catalyst. Inorganic Chemistry, 2016, 55, 488-501.	4.0	87
83	Fluid solution and solid-state electron nuclear double resonance studies of flavin model compounds and flavoenzymes. Journal of the American Chemical Society, 1984, 106, 737-746.	13.7	86
84	Effects of Hydrogen Bonding to a Bacteriochlorophyllâ^'Bacteriopheophytin Dimer in Reaction Centers fromRhodobacter sphaeroidesâ€. Biochemistry, 1996, 35, 6612-6619.	2.5	84
85	Radicals in solution studied by endor and triple resonance spectroscopy. Physics Reports, 1982, 87, 171-208.	25.6	83
86	Pulsed EPR Structure Analysis of Photosystem I Single Crystals:Â Localization of the Phylloquinone Acceptorâ€. Biochemistry, 1997, 36, 12001-12004.	2.5	82
87	Quantum chemical calculations of [NiFe] hydrogenase. Current Opinion in Chemical Biology, 2002, 6, 243-249.	6.1	81
88	The electronic structures of the S2 states of the oxygen-evolving complexes of photosystem II in plants and cyanobacteria in the presence and absence of methanol. Biochimica Et Biophysica Acta - Bioenergetics, 2011, 1807, 829-840.	1.0	81
89	Structural and Spectroscopic Features of Mixed Valent Fe ^{II} Fe ^I Complexes and Factors Related to the Rotated Configuration of Diiron Hydrogenase. Journal of the American Chemical Society, 2012, 134, 13089-13102.	13.7	81
90	Mechanism of Protection of Catalysts Supported in Redox Hydrogel Films. Journal of the American Chemical Society, 2015, 137, 5494-5505.	13.7	81

#	Article	IF	CITATIONS
91	Photosystem II single crystals studied by EPR spectroscopy at 94 GHz: The tyrosine radical YFormula. Proceedings of the National Academy of Sciences of the United States of America, 2001, 98, 6623-6628.	7.1	79
92	Reaction Coordinate Leading to H ₂ Production in [FeFe]-Hydrogenase Identified by Nuclear Resonance Vibrational Spectroscopy and Density Functional Theory. Journal of the American Chemical Society, 2017, 139, 16894-16902.	13.7	78
93	Structure, ligands and substrate coordination of the oxygen-evolving complex of photosystem II in the S2 state: a combined EPR and DFT study. Physical Chemistry Chemical Physics, 2014, 16, 11877.	2.8	77
94	Enhancing hydrogen production of microalgae by redirecting electrons from photosystem I to hydrogenase. Energy and Environmental Science, 2014, 7, 3296-3301.	30.8	77
95	Inhibition of the [NiFe] hydrogenase from Desulfovibrio vulgaris Miyazaki F by carbon monoxide: An FTIR and EPR spectroscopic study. Biochimica Et Biophysica Acta - Bioenergetics, 2010, 1797, 304-313.	1.0	76
96	Relationship between the oxidation potential and electron spin density of the primary electron donor in reaction centers from Rhodobacter sphaeroides. Proceedings of the National Academy of Sciences of the United States of America, 1997, 94, 13582-13587.	7.1	75
97	A Structural Model for the Charge Separated State in Photosystem I from the Orientation of the Magnetic Interaction Tensors. Journal of Physical Chemistry B, 2000, 104, 9728-9739.	2.6	75
98	ENDOR and ESEEM of the 15N labelled radical cations of chlorophyll a and the primary donor P700 in photosystem I. Chemical Physics, 1995, 194, 419-432.	1.9	74
99	Lightâ€Induced Excited Spin State Trapping in an Exchangeâ€Coupled Nitroxideâ€Copper(II)â€Nitroxide Cluster. Angewandte Chemie - International Edition, 2008, 47, 6897-6899.	13.8	74
100	EPR and ENDOR characterization of semiquinone anion radicals related to photosynthesis. Magnetic Resonance in Chemistry, 1995, 33, S81-S93.	1.9	72
101	DFT calculations of the electronic structure of the paramagnetic states Ni-A, Ni-B and Ni-C of [NiFe] hydrogenase. Physical Chemistry Chemical Physics, 2001, 3, 2668-2675.	2.8	72
102	A gas breathing hydrogen/air biofuel cell comprising a redox polymer/hydrogenase-based bioanode. Nature Communications, 2018, 9, 4715.	12.8	71
103	Molecular orbital investigation of dimer formations of bacteriochlorophyll a. Model configurations for the primary donor of photosynthesis. Chemical Physics, 1986, 107, 185-196.	1.9	69
104	Spectroscopic Investigations of [FeFe] Hydrogenase Maturated with [⁵⁷ Fe ₂ (adt)(CN) ₂ (CO) ₄] ^{2–} . Journal of the American Chemical Society, 2015, 137, 8998-9005.	13.7	69
105	Atomic-Scale Explanation of O ₂ Activation at the Au–TiO ₂ Interface. Journal of the American Chemical Society, 2018, 140, 18082-18092.	13.7	69
106	A solution ENDOR sensitivity study of various nuclei in organic radicals. The Journal of Physical Chemistry, 1981, 85, 1202-1219.	2.9	68
107	Geometry of the Hydrogen Bonds to the Primary Quinone <mmi:math altimg="sil.gir" display="inline<br">overflow="scroll" xmlns:xocs="http://www.elsevier.com/xml/xocs/dtd" xmlns:xs="http://www.w3.org/2001/XMLSchema" xmlns:xsi="http://www.w3.org/2001/XMLSchema-instance" xmlns="http://www.elsevier.com/xml/ja/dtd"</mmi:math>	0.5	68
108	xmhnsja="http://www.elsevier.com/xml/ja/dtd" xmhnsmml="http://www.w3.org/1990/Math/Math/Mc" The first tyrosyl radical intermediate formed in the S2–S3 transition of photosystem II. Physical Chemistry Chemical Physics, 2014, 16, 11901.	2.8	68

7

#	Article	IF	CITATIONS
109	Charge Recombination Fluorescence in Photosystem I Reaction Centers fromChlamydomonas reinhardtii. Journal of Physical Chemistry B, 2005, 109, 5903-5911.	2.6	66
110	A tunable general purpose Q-band resonator for CW and pulse EPR/ENDOR experiments with large sample access and optical excitation. Journal of Magnetic Resonance, 2012, 214, 237-243.	2.1	66
111	Species-specific Differences of the Spectroscopic Properties of P700. Journal of Biological Chemistry, 2003, 278, 46760-46771.	3.4	65
112	In vivo liquid solution ENDOR and TRIPLE resonance of bacterial photosynthetic reaction centers of Rhodopseudomonas sphaeroides R-26. Journal of the American Chemical Society, 1981, 103, 4635-4637.	13.7	64
113	Transient EPR spectroscopy of the charge separated state P+Qâ^' in photosynthetic reaction centers. Comparison of Zn-substituted Rhodobacter sphaeroides R-26 and Photosystem I. Biochimica Et Biophysica Acta - Bioenergetics, 1993, 1142, 23-35.	1.0	64
114	Differences in the binding of the primary quinone receptor in Photosystem I and reaction centres of Rhodobacter sphaeroides-R26 studied with transient EPR spectroscopy. Chemical Physics, 1995, 194, 349-359.	1.9	64
115	g- andA-Tensor Calculations in the Zero-Order Approximation for Relativistic Effects of Ni Complexes and Ni(CO)3H as Model Complexes for the Active Center of [NiFe]-Hydrogenase. Journal of Physical Chemistry A, 2001, 105, 416-425.	2.5	64
116	Probing hydrogen bonding to quinone anion radicals by 1H and 2H ENDOR spectroscopy at 35 GHz. Chemical Physics, 2003, 294, 401-413.	1.9	64
117	Spectroscopic Characterization of the Bridging Amine in the Active Site of [FeFe] Hydrogenase Using Isotopologues of the H-Cluster. Journal of the American Chemical Society, 2015, 137, 12744-12747.	13.7	64
118	ESR, ENDOR and TRIPLE resonance studies of the primary donor radical cation P960+• in the photosynthetic bacterium Rhodopseudomonas viridis. Chemical Physics Letters, 1988, 148, 377-385.	2.6	63
119	The First State in the Catalytic Cycle of the Water-Oxidizing Enzyme: Identification of a Water-Derived μ-Hydroxo Bridge. Journal of the American Chemical Society, 2017, 139, 14412-14424.	13.7	63
120	Spectroscopic and Computational Evidence that [FeFe] Hydrogenases Operate Exclusively with CO-Bridged Intermediates. Journal of the American Chemical Society, 2020, 142, 222-232.	13.7	63
121	2D ESEEM of the 15N-Labeled Radical Cations of Bacteriochlorophyll a and of the Primary Donor in Reaction Centers of Rhodobacter sphaeroides. The Journal of Physical Chemistry, 1995, 99, 436-448.	2.9	62
122	Single crystal EPR studies of the oxidized active site of [NiFe] hydrogenase from Desulfovibrio vulgaris Miyazaki F. Journal of Biological Inorganic Chemistry, 2000, 5, 36-44.	2.6	62
123	Structure of the Tyrosyl Biradical in Mouse R2 Ribonucleotide Reductase from Highâ€Field PELDOR. Angewandte Chemie - International Edition, 2008, 47, 1224-1227.	13.8	62
124	Artificial Photosynthesis for Solar Fuels – an Evolving Research Field within AMPEA, a Joint Programme of the European Energy Research Alliance. Green, 2013, 3, .	0.4	62
125	Pigmentâ^'Protein Interactions in Bacterial Reaction Centers and Their Influence on Oxidation Potential and Spin Density Distribution of the Primary Donor. Journal of Physical Chemistry B, 2002, 106, 3226-3236.	2.6	61
126	Dimanganese catalase—spectroscopic parameters from broken-symmetry density functional theory of the superoxidized MnIII/MnIV state. Journal of Biological Inorganic Chemistry, 2005, 10, 231-238.	2.6	61

#	Article	IF	CITATIONS
127	Spectroelectrochemical Study of the [NiFe] Hydrogenase from Desulfovibrio vulgaris Miyazaki F in Solution and Immobilized on Biocompatible Gold Surfaces. Journal of Physical Chemistry B, 2009, 113, 15344-15351.	2.6	61
128	Direct Comparison of the Performance of a Bioâ€inspired Synthetic Nickel Catalyst and a [NiFe]â€Hydrogenase, Both Covalently Attached to Electrodes. Angewandte Chemie - International Edition, 2015, 54, 12303-12307.	13.8	61
129	Time-resolved EPR of the radical pair P865+.QAâ^'. in bacterial reaction centers. Observations of transient nutations, quantum beats and envelope modulation effects. Chemical Physics Letters, 1994, 226, 349-358.	2.6	60
130	Pulsed EPR measurement of the distance between P680 +· and QA â^'· in photosystem II. FEBS Letters, 1997, 414, 454-456.	2.8	60
131	Multifrequency EPR Investigation of Dimanganese Catalase and Related Mn(III)Mn(IV) Complexes. Journal of Physical Chemistry B, 2003, 107, 1242-1250.	2.6	60
132	De novo design of a non-natural fold for an iron–sulfur protein: Alpha-helical coiled-coil with a four-iron four-sulfur cluster binding site in its central core. Biochimica Et Biophysica Acta - Bioenergetics, 2010, 1797, 406-413.	1.0	60
133	Observation of the FeCN and FeCO Vibrations in the Active Site of [NiFe] Hydrogenase by Nuclear Resonance Vibrational Spectroscopy. Angewandte Chemie - International Edition, 2013, 52, 724-728.	13.8	60
134	Artificial photosynthesis: understanding water splitting in nature. Interface Focus, 2015, 5, 20150009.	3.0	60
135	Transient EPR spectroscopy of perdeuterated Zn-substituted reaction centres of Rhodobacter sphaeroides R-26. Chemical Physics Letters, 1993, 212, 561-568.	2.6	59
136	W-band ELDOR-detected NMR (EDNMR) spectroscopy as a versatile technique for the characterisation of transition metal–ligand interactions. Molecular Physics, 2013, 111, 2788-2808.	1.7	59
137	Molecular orbital study of the primary electron donor P700 of photosystem I based on a recent X-ray single crystal structure analysis. Chemical Physics, 2003, 294, 483-499.	1.9	58
138	Redox active iron nitrosyl units in proton reduction electrocatalysis. Nature Communications, 2014, 5, 3684.	12.8	58
139	Electron Spinâ^'Lattice Relaxation of the S0 State of the Oxygen-Evolving Complex in Photosystem II and of Dinuclear Manganese Model Complexes. Biochemistry, 2005, 44, 9368-9374.	2.5	57
140	Electronic structure of the unique [4Fe-3S] cluster in O ₂ -tolerant hydrogenases characterized by ⁵⁷ Fe Mössbauer and EPR spectroscopy. Proceedings of the National Academy of Sciences of the United States of America, 2013, 110, 483-488.	7.1	57
141	Electronic Structure of a Transient Histidine Radical in Liquid Aqueous Solution:Â EPR Continuous-Flow Studies and Density Functional Calculations. Journal of Physical Chemistry A, 1999, 103, 1283-1290.	2.5	56
142	The Basic Properties of the Electronic Structure of the Oxygen-evolving Complex of Photosystem II Are Not Perturbed by Ca2+ Removal. Journal of Biological Chemistry, 2012, 287, 24721-24733.	3.4	56
143	Theoretical Spectroscopy of the Ni ^{II} Intermediate States in the Catalytic Cycle and the Activation of [NiFe] Hydrogenases. ChemBioChem, 2013, 14, 1898-1905.	2.6	56
144	Models of the Ni-L and Ni-SI _a States of the [NiFe]-Hydrogenase Active Site. Inorganic Chemistry, 2016, 55, 419-431.	4.0	56

#	Article	IF	CITATIONS
145	Intercluster Redox Coupling Influences Protonation at the H-cluster in [FeFe] Hydrogenases. Journal of the American Chemical Society, 2017, 139, 15122-15134.	13.7	56
146	EPR and ENDOR studies of the water oxidizing complex of Photosystem II. Photosynthesis Research, 1996, 48, 227-237.	2.9	55
147	Pulsed ENDOR at 95 GHz on the Primary Acceptor Ubisemiquinone in Photosynthetic Bacterial Reaction Centers and Related Model Systems. Journal of Physical Chemistry B, 1998, 102, 4648-4657.	2.6	55
148	The electronic structure of the catalytic intermediate Ni-C in [NiFe] and [NiFeSe] hydrogenasesElectronic Supplementary Information available. See http://www.rsc.org/suppdata/cp/b1/b105723p/. Physical Chemistry Chemical Physics, 2001, 3, 5115-5120.	2.8	55
149	Rapid and Reversible Reactions of [NiFe]-Hydrogenases with Sulfide. Journal of the American Chemical Society, 2006, 128, 7448-7449.	13.7	55
150	Electronic Structure of a Weakly Antiferromagnetically Coupled Mn ^{II} Mn ^{III} Model Relevant to Manganese Proteins: A Combined EPR, ⁵⁵ Mn-ENDOR, and DFT Study. Inorganic Chemistry, 2011, 50, 8238-8251.	4.0	55
151	Structural studies of the primary donor cation radical P870+{middle dot} in reaction centers of Rhodospirillum rubrum by electron-nuclear double resonance in solution. Proceedings of the National Academy of Sciences of the United States of America, 1984, 81, 1401-1405.	7.1	54
152	Orientation-Selected 95 GHz High-Field ENDOR Spectroscopy of Randomly Oriented Plastoquinone Anion Radicals. Journal of Magnetic Resonance Series A, 1995, 116, 59-66.	1.6	54
153	Five-coordinate Mn ^{IV} intermediate in the activation of nature's water splitting cofactor. Proceedings of the National Academy of Sciences of the United States of America, 2019, 116, 16841-16846.	7.1	54
154	Transient EPR and Absorption Studies of Carotenoid Triplet Formation in Purple Bacterial Antenna Complexes. Journal of Physical Chemistry B, 2001, 105, 5525-5535.	2.6	53
155	Spectroscopic characterization of the key catalytic intermediate Ni–C in the O2-tolerant [NiFe] hydrogenase I from Aquifex aeolicus: evidence of a weakly bound hydride. Chemical Communications, 2012, 48, 823-825.	4.1	53
156	Unique Spectroscopic Properties of the H-Cluster in a Putative Sensory [FeFe] Hydrogenase. Journal of the American Chemical Society, 2018, 140, 1057-1068.	13.7	53
157	A fully protected hydrogenase/polymer-based bioanode for high-performance hydrogen/glucose biofuel cells. Nature Communications, 2018, 9, 3675.	12.8	53
158	Preventing the coffee-ring effect and aggregate sedimentation by <i>in situ</i> gelation of monodisperse materials. Chemical Science, 2018, 9, 7596-7605.	7.4	53
159	15N electron nuclear double resonance of the primary donor cation radical P+.865 in reaction centers of Rhodopseudomonas sphaeroides: additional evidence for the dimer model Proceedings of the National Academy of Sciences of the United States of America, 1984, 81, 7792-7796.	7.1	52
160	Pulsed EPR experiments on radical pairs in photosynthesis: Comparison of the donor-acceptor distances in photosystem I and bacterial reaction centers. Zeitschrift Fur Elektrotechnik Und Elektrochemie, 1996, 100, 2041-2044.	0.9	51
161	Electronic and Vibronic Coupling of the Special Pair of Bacteriochlorophylls in Photosynthetic Reaction Centers from Wild-Type and Mutant Strains ofRhodobacter Sphaeroides. Journal of Physical Chemistry B, 2002, 106, 11859-11869.	2.6	49
162	Direct observation of structurally encoded metal discrimination and ether bond formation in a heterodinuclear metalloprotein. Proceedings of the National Academy of Sciences of the United States of America, 2013, 110, 17189-17194.	7.1	49

#	Article	IF	CITATIONS
163	The catalytic cycle of [FeFe] hydrogenase: A tale of two sites. Coordination Chemistry Reviews, 2021, 449, 214191.	18.8	49
164	Single crystal EPR study of the Ni center of NiFe hydrogenase. Chemical Physics Letters, 1996, 256, 518-524.	2.6	48
165	High-field EPR, ENDOR and ELDOR on bacterial photosynthetic reaction centers. Applied Magnetic Resonance, 2007, 31, 59-98.	1.2	48
166	SEIRA Spectroscopy of the Electrochemical Activation of an Immobilized [NiFe] Hydrogenase under Turnover and Nonâ€Turnover Conditions. Angewandte Chemie - International Edition, 2011, 50, 2632-2634.	13.8	48
167	Chalcogenide substitution in the [2Fe] cluster of [FeFe]-hydrogenases conserves high enzymatic activity. Dalton Transactions, 2017, 46, 16947-16958.	3.3	48
168	Engineering an [FeFe]-Hydrogenase: Do Accessory Clusters Influence O ₂ Resistance and Catalytic Bias?. Journal of the American Chemical Society, 2018, 140, 5516-5526.	13.7	48
169	Observation of deuterium quadrupole splittings of aromatic free radicals in liquid crystals by ENDOR and TRIPLE resonance. Journal of Chemical Physics, 1977, 66, 2074-2078.	3.0	47
170	Evaluation of 2D-ESEEM data of 15N-labeled radical cations of the primary donor P700 in photosystem I and chlorophyll a. Chemical Physics Letters, 1996, 251, 193-203.	2.6	47
171	Electronic Structure of the Cysteine Thiyl Radical:  A DFT and Correlated ab Initio Study. Journal of the American Chemical Society, 2004, 126, 2237-2246.	13.7	47
172	Structural and dynamical characteristics of trehalose and sucrose matrices at different hydration levels as probed by FTIR and high-field EPR. Physical Chemistry Chemical Physics, 2014, 16, 9831-9848.	2.8	47
173	Sulfide Protects [FeFe] Hydrogenases From O ₂ . Journal of the American Chemical Society, 2018, 140, 9346-9350.	13.7	47
174	Computational study of the electronic structure and magnetic properties of the Ni–C state in [NiFe] hydrogenases including the second coordination sphere. Journal of Biological Inorganic Chemistry, 2012, 17, 1269-1281.	2.6	46
175	Protein Immobilization Capabilities of Sucrose and Trehalose Glasses: The Effect of Protein/Sugar Concentration Unraveled by High-Field EPR. Journal of Physical Chemistry Letters, 2016, 7, 4871-4877.	4.6	46
176	High-field ELDOR-detected NMR study of a nitroxide radical in disordered solids: Towards characterization of heterogeneity of microenvironments in spin-labeled systems. Journal of Magnetic Resonance, 2014, 242, 203-213.	2.1	45
177	Alkali and H ENDOR on aromatic ion pairs in solution. An INDO approach. The Journal of Physical Chemistry, 1979, 83, 3402-3413.	2.9	44
178	Probing the surrounding of a cobalt(II) porphyrin and its superoxo complex by EPR techniques. Applied Magnetic Resonance, 2001, 20, 35-70.	1.2	44
179	EPR experiments to elucidate the structure of the ready and unready states of the [NiFe] hydrogenase of Desulfovibrio vulgaris Miyazaki F. Biochemical Society Transactions, 2005, 33, 7-11.	3.4	44
180	The Iron-Oxygen Reconstitution Reaction in Protein R2-Tyr-177 Mutants of Mouse Ribonucleotide Reductase. Journal of Biological Chemistry, 1999, 274, 17696-17704.	3.4	43

#	Article	IF	CITATIONS
181	Hyperfine structure of the photoexcited triplet state 3P680 in plant PS II reaction centres as determined by pulse ENDOR spectroscopy. Biochimica Et Biophysica Acta - Bioenergetics, 2003, 1605, 35-46.	1.0	43
182	Protein thiyl radicals in disordered systems: A comparative EPR study at low temperature. Physical Chemistry Chemical Physics, 2003, 5, 2442-2453.	2.8	43
183	Spin distribution of the H-cluster in the Hox–CO state of the [FeFe]Âhydrogenase from Desulfovibrio desulfuricans: HYSCORE and ENDOR study of 14N and 13C nuclear interactions. Journal of Biological Inorganic Chemistry, 2009, 14, 301-313.	2.6	43
184	Electronic Structure of the Quinone Radical Anion A ₁ ^{•â^'} of Photosystem I Investigated by Advanced Pulse EPR and ENDOR Techniques. Journal of Physical Chemistry B, 2009, 113, 10367-10379.	2.6	42
185	Interplay between CN [–] Ligands and the Secondary Coordination Sphere of the H-Cluster in [FeFe]-Hydrogenases. Journal of the American Chemical Society, 2017, 139, 18222-18230.	13.7	42
186	The Quinone Acceptor A1 in Photosystem I:  Binding Site, and Comparison to QA in Purple Bacteria Reaction Centers. Journal of Physical Chemistry B, 1998, 102, 8278-8287.	2.6	41
187	Protein–cofactor interactions in bacterial reaction centers from Rhodobacter sphaeroides R-26: Effect of hydrogen bonding on the electronic and geometric structure of the primary quinone. A density functional theory study. Physical Chemistry Chemical Physics, 2006, 8, 5659-5670.	2.8	41
188	EPR, ENDOR, and TRIPLE resonance studies of modified bacteriochlorophyll cation radicals. The Journal of Physical Chemistry, 1994, 98, 354-363.	2.9	40
189	An Improved TM110 ENDOR Cavity for the Investigation of Transition Metal Complexes. Journal of Magnetic Resonance Series A, 1994, 109, 172-176.	1.6	40
190	Incorporation of a high potential quinone reveals that electron transfer in Photosystem I becomes highly asymmetric at low temperature. Photochemical and Photobiological Sciences, 2012, 11, 946-956.	2.9	40
191	Semisynthetic Hydrogenases Propel Biological Energy Research into a New Era. Joule, 2017, 1, 61-76.	24.0	40
192	ESR, NMR, and ENDOR studies of partially deuterated phenyl substituted anthracenespisigma. Delocalization. Journal of the American Chemical Society, 1977, 99, 4278-4286.	13.7	39
193	Pulse EPR and ENDOR studies of light-induced radicals and triplet states in photosystem II of oxygenic photosynthesis. Physical Chemistry Chemical Physics, 2002, 4, 5539-5545.	2.8	39
194	Multifrequency EPR analysis of the dimanganese cluster of the putative sulfate thiohydrolase SoxB of Paracoccus pantotrophus. Journal of Biological Inorganic Chemistry, 2005, 10, 636-642.	2.6	39
195	Electron-nuclear double resonance. Photosynthesis Research, 2009, 102, 391-401.	2.9	39
196	Zinc-Bacteriochlorophyllide Dimers in de Novo Designed Four-Helix Bundle Proteins. A Model System for Natural Light Energy Harvesting and Dissipation. Journal of the American Chemical Society, 2011, 133, 9526-9535.	13.7	39
197	Artificially maturated [FeFe] hydrogenase from Chlamydomonas reinhardtii: a HYSCORE and ENDOR study of a non-natural H-cluster. Physical Chemistry Chemical Physics, 2015, 17, 5421-5430.	2.8	39
198	Artificial Maturation of the Highly Active Heterodimeric [FeFe] Hydrogenase from <i>Desulfovibrio desulfuricans</i> ATCC 7757. Israel Journal of Chemistry, 2016, 56, 852-863.	2.3	39

#	Article	IF	CITATIONS
199	Title is missing!. Photosynthesis Research, 1998, 55, 189-197.	2.9	38
200	Structural and functional characterization of the hydrogenase-maturation HydF protein. Nature Chemical Biology, 2017, 13, 779-784.	8.0	38
201	Investigating the Kinetic Competency of <i>Cr</i> HydA1 [FeFe] Hydrogenase Intermediate States via Time-Resolved Infrared Spectroscopy. Journal of the American Chemical Society, 2019, 141, 16064-16070.	13.7	38
202	The H2 sensor of Ralstonia eutropha: biochemical and spectroscopic analysis of mutant proteins modified at a conserved glutamine residue close to the [NiFe] active site. Journal of Biological Inorganic Chemistry, 2002, 7, 897-908.	2.6	37
203	Pulse EPR, 55Mn-ENDOR and ELDOR-detected NMR of the S2-state of the oxygen evolving complex in Photosystem II. Photosynthesis Research, 2005, 84, 347-353.	2.9	37
204	Temperature-Dependent Exchange Interaction in Molecular Magnets Cu(hfac) ₂ L ^R Studied by EPR: Methodology and Interpretations. Inorganic Chemistry, 2011, 50, 10204-10212.	4.0	37
205	Electronic Structural Flexibility of Heterobimetallic Mn/Fe Cofactors: R2lox and R2c Proteins. Journal of the American Chemical Society, 2014, 136, 13399-13409.	13.7	37
206	ENDOR and pulsed EPR studies of photosynthetic reaction centers: Protein ofactor interactions. Zeitschrift Fur Elektrotechnik Und Elektrochemie, 1996, 100, 2036-2040.	0.9	36
207	Quadrupole parameters of nitrogen nuclei in the cation radical P700.+ determined by ESEEM of single crystals of phtosystem I. Chemical Physics Letters, 1996, 257, 197-206.	2.6	36
208	Characterization of radical intermediates in laccase-mediator systems. A multifrequency EPR, ENDOR and DFT/PCM investigation. Physical Chemistry Chemical Physics, 2008, 10, 7284.	2.8	36
209	A [RuRu] Analogue of an [FeFe]-Hydrogenase Traps the Key Hydride Intermediate of the Catalytic Cycle. Angewandte Chemie - International Edition, 2018, 57, 5429-5432.	13.8	36
210	Protein thiyl radicals directly observed by EPR spectroscopy. Archives of Biochemistry and Biophysics, 2002, 403, 141-144.	3.0	35
211	The S1YZ? metalloradical intermediate in photosystem II: an X- and W-band EPR study. Physical Chemistry Chemical Physics, 2004, 6, 4859.	2.8	35
212	Probing intermediates in the activation cycle of [NiFe] hydrogenase by infrared spectroscopy: the Ni-SIr state and its light sensitivity. Journal of Biological Inorganic Chemistry, 2009, 14, 1227-1241.	2.6	35
213	FTIR study on the light sensitivity of the [NiFe] hydrogenase from Desulfovibrio vulgaris Miyazaki F: Ni–C to Ni–L photoconversion, kinetics of proton rebinding and H/D isotope effect. Physical Chemistry Chemical Physics, 2009, 11, 8680.	2.8	35
214	High-Field Dipolar Electron Paramagnetic Resonance (EPR) Spectroscopy of Nitroxide Biradicals for Determining Three-Dimensional Structures of Biomacromolecules in Disordered Solids. Journal of Physical Chemistry B, 2011, 115, 11950-11963.	2.6	35
215	Cofactor composition and function of a H ₂ -sensing regulatory hydrogenase as revealed by Mössbauer and EPR spectroscopy. Chemical Science, 2015, 6, 4495-4507.	7.4	35
216	ELDOR-detected NMR: A general and robust method for electron-nuclear hyperfine spectroscopy?. Journal of Magnetic Resonance, 2017, 280, 63-78.	2.1	35

#	Article	IF	CITATIONS
217	Dual properties of a hydrogen oxidation Ni-catalyst entrapped within a polymer promote self-defense against oxygen. Nature Communications, 2018, 9, 864.	12.8	35
218	Phylloquinone and Related Radical Anions Studied by Pulse Electron Nuclear Double Resonance Spectroscopy at 34 GHz and Density Functional Theory. Journal of Physical Chemistry B, 2006, 110, 11549-11560.	2.6	34
219	Crucial Role of Paramagnetic Ligands for Magnetostructural Anomalies in "Breathing Crystals― Inorganic Chemistry, 2012, 51, 9385-9394.	4.0	34
220	The Radical Pair State in Photosystem I Single Crystals:  Orientation Dependence of the Transient Spin-Polarized EPR Spectra. Journal of Physical Chemistry B, 1998, 102, 8266-8277.	2.6	33
221	Wavelength dependence of the photo-induced conversion of the Ni–C to the Ni–L redox state in the [NiFe] hydrogenase of Desulfovibrio vulgaris Miyazaki F. Physical Chemistry Chemical Physics, 2003, 5, 5507-5513.	2.8	33
222	Electronâ^'Electron Double Resonance-Detected NMR to Measure Metal Hyperfine Interactions: ⁶¹ Ni in the Niâ^'B State of the [NiFe] Hydrogenase of <i>Desulfovibrio vulgaris</i> Miyazaki F. Journal of the American Chemical Society, 2008, 130, 2402-2403.	13.7	33
223	Endor and triple resonance in solutions of the chlorophyll a and bis(chlorophyll)cyclophane radical cations. Chemical Physics Letters, 1986, 132, 467-473. Protein-Cofactor Interactions in Bacterial Reaction Centers from Rhodobacter sphaeroides R-26: I.	2.6	32
224	Identification of the ENDOR Lines Associated with the Hydrogen Bonds to the Primary Quinone <mml:math <br="" altimg="si12.gif" display="inline" overflow="scroll">xmlns:xocs="http://www.elsevier.com/xml/xocs/dtd" xmlns:xs="http://www.w3.org/2001/XMLSchema" xmlns:xsi="http://www.w3.org/2001/XMLSchema-instance" xmlns="http://www.elsevier.com/xml/ja/dtd"</mml:math>	0.5	32
225	xmlns:ia="http://www.elsevier.com/xml/ia/dtd" xmlns:mnl="http://www_Biophysical Journal, 2006, 90, Characterization of a cyanobacterial-like uptake [NIFe]Ahydrogenase: EPR and FfiR spectroscopic studies of the enzyme from Acidithiobacillus ferrooxidans. Journal of Biological Inorganic Chemistry, 2007, 12, 212-233.	2.6	32
226	Key Hydride Vibrational Modes in [NiFe] Hydrogenase Model Compounds Studied by Resonance Raman Spectroscopy and Density Functional Calculations. Inorganic Chemistry, 2012, 51, 11787-11797.	4.0	32
227	Direct Detection of the Terminal Hydride Intermediate in [FeFe] Hydrogenase by NMR Spectroscopy. Journal of the American Chemical Society, 2018, 140, 3863-3866.	13.7	32
228	The radical SAM protein HemW is a heme chaperone. Journal of Biological Chemistry, 2018, 293, 2558-2572.	3.4	32
229	His-Ligation to the [4Fe–4S] Subcluster Tunes the Catalytic Bias of [FeFe] Hydrogenase. Journal of the American Chemical Society, 2019, 141, 472-481.	13.7	32
230	Transient and pulsed EPR spectroscopy on the radical pair state P 865 +. Q A â''. to study light-induced changes in bacterial reaction centers. Applied Magnetic Resonance, 1997, 13, 517-529.	1.2	31
231	Spin-Density Distribution of the Carotenoid Triplet State in the Peridinin-Chlorophyll-Protein Antenna. A Q-Band Pulse Electron-Nuclear Double Resonance and Density Functional Theory Study. Journal of the American Chemical Society, 2007, 129, 15442-15443.	13.7	31
232	Trehalose matrix effects on charge-recombination kinetics in Photosystem I of oxygenic photosynthesis at different dehydration levels. Biochimica Et Biophysica Acta - Bioenergetics, 2016, 1857, 1440-1454.	1.0	31
233	Influence of hydrogen bonds on the electronicg-tensor and13C-hyperfine tensors of13C-labeled ubiquinones — EPR and ENDOR study. Applied Magnetic Resonance, 1998, 14, 255-274.	1.2	30
234	Orientation-selected ENDOR of the active center in Chromatium vinosum [NiFe] hydrogenase in the oxidized "ready" state. Journal of Biological Inorganic Chemistry, 1999, 4, 379-389.	2.6	30

#	Article	IF	CITATIONS
235	Electron Paramagnetic Resonance Studies of Zinc-Substituted Reaction Centers from Rhodopseudomonas viridis. Biochemistry, 1999, 38, 11773-11787.	2.5	30
236	Determination of the distance between Yoxâ‹ Z and Qâ^'â‹ A in photosystem II by pulsed EPR spectroscopy on light-induced radical pairs. FEBS Letters, 1999, 442, 79-82.	2.8	30
237	Characterization of de novo synthesized four-helix bundle proteins with metalloporphyrin cofactors. Physical Chemistry Chemical Physics, 2001, 3, 4082-4090.	2.8	30
238	High-frequency EPR studies on cofactor radicals in photosystem I. Applied Magnetic Resonance, 2001, 21, 363-379.	1.2	30
239	Molecular Dynamics of QA-• and QB-• in Photosynthetic Bacterial Reaction Centers Studied by Pulsed High-Field EPR at 95 GHz. Journal of Physical Chemistry B, 2002, 106, 9454-9462.	2.6	30
240	Empirical and computational design of iron-sulfur cluster proteins. Biochimica Et Biophysica Acta - Bioenergetics, 2012, 1817, 1256-1262.	1.0	30
241	3 mm EPR investigation of the primary donor cation radical in single crystals of Rhodobacter sphaeroides R-26 reaction centers. Chemical Physics Letters, 1991, 185, 381-386.	2.6	29
242	Electron Paramagnetic Resonance and Electron Nuclear Double Resonance Investigation of the Diradical Bis(α-iminopyridinato)zinc Complex. Inorganic Chemistry, 2009, 48, 2626-2632.	4.0	29
243	[Fe4S4]- and [Fe3S4]-cluster formation in synthetic peptides. Biochimica Et Biophysica Acta - Bioenergetics, 2011, 1807, 1414-1422.	1.0	29
244	Orientation and Function of a Membrane-Bound Enzyme Monitored by Electrochemical Surface-Enhanced Infrared Absorption Spectroscopy. Journal of Physical Chemistry Letters, 2013, 4, 2794-2798.	4.6	29
245	In search of metal hydrides: an X-ray absorption and emission study of [NiFe] hydrogenase model complexes. Physical Chemistry Chemical Physics, 2016, 18, 10688-10699.	2.8	29
246	Endor studies of [6]helicene anion radical. Tetrahedron, 1979, 35, 905-907.	1.9	28
247	Structure of a Transient Neutral Histidine Radical in Solution:Â EPR Continuous-Flow Studies in a Ti3+/EDTAâ°'Fenton System and Density Functional Calculations. Journal of Physical Chemistry A, 2000, 104, 9144-9152.	2.5	28
248	Hydrogen Bonding Affects the [NiFe] Active Site of Desulfovibrio vulgaris Miyazaki F Hydrogenase:  A Hyperfine Sublevel Correlation Spectroscopy and Density Functional Theory Study. Journal of Physical Chemistry B, 2006, 110, 8142-8150.	2.6	28
249	EPR/ENDOR, Mössbauer, and Quantum-Chemical Investigations of Diiron Complexes Mimicking the Active Oxidized State of [FeFe]Hydrogenase. Inorganic Chemistry, 2012, 51, 8617-8628.	4.0	28
250	Structural Insight into the Complex of Ferredoxin and [FeFe] Hydrogenase from <i>Chlamydomonas reinhardtii</i> . ChemBioChem, 2015, 16, 1663-1669.	2.6	28
251	Spectroscopic and biochemical insight into an electron-bifurcating [FeFe] hydrogenase. Journal of Biological Inorganic Chemistry, 2020, 25, 135-149.	2.6	28
252	Suppressing hydrogen peroxide generation to achieve oxygen-insensitivity of a [NiFe] hydrogenase in redox active films. Nature Communications, 2020, 11, 920.	12.8	28

#	Article	IF	CITATIONS
253	Photosystem II single crystals studied by transient EPR: the light-induced triplet state. Biochimica Et Biophysica Acta - Bioenergetics, 2003, 1605, 47-54.	1.0	27
254	Probing Mode and Site of Substrate Water Binding to the Oxygen-Evolving Complex in the S ₂ State of Photosystem II by ¹⁷ O-HYSCORE Spectroscopy. Journal of the American Chemical Society, 2008, 130, 786-787.	13.7	27
255	Dynamic mixing processes in spin triads of "breathing crystals―Cu(hfac)2LR: a multifrequency EPR study at 34, 122 and 244 GHz. Physical Chemistry Chemical Physics, 2009, 11, 6654.	2.8	27
256	Orientation Resolving Dipolar High-Field EPR Spectroscopy on Disordered Solids: II. Structure of Spin-Correlated Radical Pairs in Photosystem I. Journal of Physical Chemistry B, 2013, 117, 11184-11199.	2.6	27
257	In Situ EPR Characterization of a Cobalt Oxide Water Oxidation Catalyst at Neutral pH. Catalysts, 2019, 9, 926.	3.5	27
258	Chemical assembly of multiple metal cofactors: The heterologously expressed multidomain [FeFe]-hydrogenase from Megasphaera elsdenii. Biochimica Et Biophysica Acta - Bioenergetics, 2016, 1857, 1734-1740.	1.0	26
259	Light and Temperature Control of the Spin State of Bis(<i>p</i> -methoxyphenyl)carbene: A Magnetically Bistable Carbene. Journal of the American Chemical Society, 2016, 138, 1622-1629.	13.7	26
260	A novel versatile microbiosensor for local hydrogen detection by means of scanning photoelectrochemical microscopy. Biosensors and Bioelectronics, 2017, 94, 433-437.	10.1	26
261	The bacteriopheophytin a anion radical. A solution endor and triple resonance study. Chemical Physics Letters, 1981, 84, 33-38.	2.6	25
262	Multiple magnetic resonance studies on organic molecules in their ground and excited states. The Journal of Physical Chemistry, 1982, 86, 4491-4507.	2.9	25
263	Generation and Electron Paramagnetic Resonance Spin Trapping Detection of Thiyl Radicals in Model Proteins and in the R1 Subunit of Escherichia coli Ribonucleotide Reductase. Archives of Biochemistry and Biophysics, 2002, 397, 57-68.	3.0	25
264	Carbon-13 ENDOR studies of organic doublet and triplet state molecules. Journal of the American Chemical Society, 1978, 100, 2292-2299.	13.7	24
265	ENDOR studies of substituted chlorophyll cation radicals. Spectrochimica Acta - Part A: Molecular and Biomolecular Spectroscopy, 1998, 54, 1141-1156.	3.9	24
266	Comparison of the membrane-bound [NiFe] hydrogenases from R. eutropha H16 and D. vulgaris Miyazaki F in the oxidized ready state by pulsed EPR. Physical Chemistry Chemical Physics, 2010, 12, 2139.	2.8	24
267	EPR Spectroscopy and the Electronic Structure of the Oxygen-Evolving Complex of Photosystem II. Applied Magnetic Resonance, 2013, 44, 691-720.	1.2	24
268	Pressure and Temperature Effects on the Activity and Structure of the Catalytic Domain of Human MT1-MMP. Biophysical Journal, 2015, 109, 2371-2381.	0.5	24
269	Divergent assembly mechanisms of the manganese/iron cofactors in R2lox and R2c proteins. Journal of Inorganic Biochemistry, 2016, 162, 164-177.	3.5	24
270	Fluorine and proton ENDOR of aromatic radicals in solution. Chemical Physics, 1975, 8, 371-383.	1.9	23

#	Article	IF	CITATIONS
271	14N and 1H electron nuclear multiple resonance experiments on bacteriochlorophyll a anion radicals in solution. Chemical Physics Letters, 1981, 81, 235-241.	2.6	23
272	Electron paramagnetic resonance and electron nuclear double resonance spectroscopy of a heme protein maquette. Chemical Physics Letters, 2000, 323, 329-339.	2.6	23
273	ChlorophyllaRadical Ions:Â A Density Functional Study. Journal of Physical Chemistry B, 2002, 106, 5281-5288.	2.6	23
274	The primary donor cation P+ in photosynthetic reaction centers of site-directed mutants of Rhodobacter sphaeroides: g-tensor shifts revealed by high-field EPR at 360 GHz/12.8 T. Chemical Physics, 2003, 294, 371-384.	1.9	23
275	Detection of Heme Oxygenase Activity in a Library of Four-helix Bundle Proteins: Towards the de Novo Synthesis of Functional Heme Proteins. Journal of Molecular Biology, 2007, 371, 739-753.	4.2	23
276	Electronâ^'Nuclear and Electronâ^'Electron Double Resonance Spectroscopies Show that the Primary Quinone Acceptor Q _A in Reaction Centers from Photosynthetic Bacteria <i>Rhodobacter sphaeroides</i> Remains in the Same Orientation Upon Light-Induced Reduction. Journal of Physical Chemistry B, 2010, 114, 16894-16901.	2.6	23
277	Unraveling the Electronic Properties of the Photoinduced States of the H-Cluster in the [FeFe] Hydrogenase from D. desulfuricans. European Journal of Inorganic Chemistry, 2011, 2011, 1056-1066.	2.0	23
278	A strenuous experimental journey searching forÂspectroscopic evidence of a bridging nickel–iron–hydride in [NiFe] hydrogenase. Journal of Synchrotron Radiation, 2015, 22, 1334-1344.	2.4	23
279	Design and Characterization of Phosphine Iron Hydrides: Toward Hydrogen-Producing Catalysts. Inorganic Chemistry, 2015, 54, 6928-6937.	4.0	23
280	Importance of Hydrogen Bonding in Fine Tuning the [2Fe-2S] Cluster Redox Potential of HydC from <i>Thermotoga maritima</i> . Biochemistry, 2016, 55, 4344-4355.	2.5	23
281	Heterodimeric Versus Homodimeric Structure of the Primary Electron Donor in Rhodobacter sphaeroides Reaction Centers Genetically Modified at Position M202‡. Photochemistry and Photobiology, 2000, 71, 582.	2.5	23
282	A CW and pulse EPR spectrometer operating at 122 and 244 GHz using a quasi-optical bridge and a cryogen-free 12 T superconducting magnet. Applied Magnetic Resonance, 2007, 31, 611-626.	1.2	22
283	High-field EPR on membrane proteins – Crossing the gap to NMR. Progress in Nuclear Magnetic Resonance Spectroscopy, 2013, 75, 1-49.	7.5	22
284	Nitrite Dismutase Reaction Mechanism: Kinetic and Spectroscopic Investigation of the Interaction between Nitrophorin and Nitrite. Journal of the American Chemical Society, 2015, 137, 4141-4150.	13.7	22
285	Asymmetry in the Ligand Coordination Sphere of the [FeFe] Hydrogenase Active Site Is Reflected in the Magnetic Spin Interactions of the Aza-propanedithiolate Ligand. Journal of Physical Chemistry Letters, 2019, 10, 6794-6799.	4.6	22
286	The bacteriochlorophylla cation radical revisited. An ENDOR and TRIPLE resonance study. Applied Magnetic Resonance, 1997, 13, 531-551.	1.2	21
287	Homologous expression of the <i>nrdF</i> gene of <i>Corynebacteriumâ€fammoniagenes</i> strainâ€fATCCâ€f6872 generates a manganeseâ€metallocofactor (R2F) and a stable tyrosyl radical (Y [•]) involved in ribonucleotide reduction. FEBS Journal, 2010, 277, 4849-4862.	4.7	21
288	Magnetic Properties of [FeFe]â€Hydrogenases: A Theoretical Investigation Based on Extended QM and QM/MM Models of the Hâ€Cluster and Its Surroundings. European Journal of Inorganic Chemistry, 2011, 2011, 1043-1049.	2.0	21

#	Article	IF	CITATIONS
289	Structural differences between the active sites of the Ni-A and Ni-B states of the [NiFe] hydrogenase: an approach by quantum chemistry and single crystal ENDOR spectroscopy. Physical Chemistry Chemical Physics, 2015, 17, 16204-16212.	2.8	21
290	Biomolecular EPR Meets NMR at High Magnetic Fields. Magnetochemistry, 2018, 4, 50.	2.4	21
291	Extending electron paramagnetic resonance to nanoliter volume protein single crystals using a self-resonant microhelix. Science Advances, 2019, 5, eaay1394.	10.3	21
292	Redoxâ€Polymerâ€Based Highâ€Currentâ€Density Gasâ€Diffusion H ₂ â€Oxidation Bioanode Using [I Hydrogenase from <i>Desulfovibrio desulfuricans</i> in a Membraneâ€free Biofuel Cell. Angewandte Chemie - International Edition, 2020, 59, 16506-16510.	FeFe] 13.8	21
293	Nitrogen-14 and hydrogen-1 ENDOR and TRIPLE resonance experiments of flavin and thiaflavin radical cations in liquid solution. Journal of the American Chemical Society, 1981, 103, 5567-5568.	13.7	20
294	Characterization of a de novo Designed Heme Protein by EPR and ENDOR Spectroscopy. Chemistry - A European Journal, 1999, 5, 2327-2334.	3.3	20
295	An EPR/ENDOR study of the asymmetric hydrogen bond between the quinone electron acceptor and the protein backbone in Photosystem I. Journal of Molecular Structure, 2004, 700, 233-241.	3.6	20
296	Modelling Lowâ€Potential [Fe ₄ S ₄] Clusters in Proteins. Chemistry and Biodiversity, 2008, 5, 1571-1587.	2.1	20
297	Spin Density Distribution of the Excited Triplet State of Bacteriochlorophylls. Pulsed ENDOR and DFT Studies. Journal of Physical Chemistry B, 2009, 113, 6917-6927.	2.6	20
298	Möbius–Hückel topology switching in an expanded porphyrin cation radical as studied by EPR and ENDOR spectroscopy. Physical Chemistry Chemical Physics, 2015, 17, 6644-6652.	2.8	20
299	Influence of the [4Fe–4S] cluster coordinating cysteines on active site maturation and catalytic properties of <i>C. reinhardtii</i> [FeFe]-hydrogenase. Chemical Science, 2017, 8, 8127-8137.	7.4	20
300	Electrochemical Investigations on the Inactivation of the [FeFe] Hydrogenase from <i>Desulfovibrio desulfuricans</i> by O ₂ or Light under Hydrogenâ€Producing Conditions. ChemPlusChem, 2017, 82, 540-545.	2.8	20
301	EPR Characterisation of Bis(dimethylglyoximato)-Cobalt(II) Complexes and Their Oxygen Adducts Synthesised in an X-Zeolite Matrix. Zeitschrift Fur Naturforschung - Section A Journal of Physical Sciences, 1987, 42, 970-986.	1.5	19
302	Title is missing!. Photosynthesis Research, 1998, 55, 199-205.	2.9	19
303	Pulse ENDOR studies on the radical pair P 700 +· A 1 ·â^' and the photoaccumulated quinone acceptor A 1 ·â^' of photosystem I. Applied Magnetic Resonance, 2004, 26, 5-21.	1.2	19
304	PELDOR study on the tyrosyl radicals in the R2 protein of mouse ribonucleotide reductase. Physical Chemistry Chemical Physics, 2006, 8, 58-62.	2.8	19
305	Effects of noncovalently bound quinones on the ground and triplet states of zinc chlorins in solution and bound to de novo synthesized peptides. Physical Chemistry Chemical Physics, 2006, 8, 5444-5453.	2.8	19
306	Electronic Structure of a Binuclear Nickel Complex of Relevance to [NiFe] Hydrogenase. Inorganic Chemistry, 2008, 47, 11688-11697.	4.0	19

#	Article	IF	CITATIONS
307	Advanced Electron Paramagnetic Resonance and Density Functional Theory Study of a {2Fe3S} Cluster Mimicking the Active Site of [FeFe] Hydrogenase. Journal of the American Chemical Society, 2010, 132, 17578-17587.	13.7	19
308	A Heme-based Redox Sensor in the Methanogenic Archaeon Methanosarcina acetivorans. Journal of Biological Chemistry, 2013, 288, 18458-18472.	3.4	19
309	The auxiliary [4Fe–4S] cluster of the Radical SAM heme synthase from Methanosarcina barkeri is involved in electron transfer. Chemical Science, 2016, 7, 4633-4643.	7.4	19
310	Proton, deuteron, and carbon-13 ENDOR studies of labeled bis(biphenylenyl)propenyl type radicals in isotropic solutions and in liquid crystals. Journal of the American Chemical Society, 1980, 102, 817-825.	13.7	18
311	Low-Temperature Pulsed EPR Study at 34 GHz of the Triplet States of the Primary Electron Donor P ₈₆₅ and the Carotenoid in Native and Mutant Bacterial Reaction Centers of <i>Rhodobacter sphaeroides</i> . Biochemistry, 2007, 46, 14782-14794.	2.5	18
312	Spectroscopic and Electrochemical Characterization of the [NiFeSe] Hydrogenase from <i>Desulfovibrio vulgaris</i> Miyazaki F: Reversible Redox Behavior and Interactions between Electron Transfer Centers. ChemBioChem, 2013, 14, 1714-1719.	2.6	18
313	Rational redesign of the ferredoxin-NADP+-oxido-reductase/ferredoxin-interaction for photosynthesis-dependent H2-production. Biochimica Et Biophysica Acta - Bioenergetics, 2018, 1859, 253-262.	1.0	18
314	Cryo-EM photosystem I structure reveals adaptation mechanisms to extreme high light in Chlorella ohadii. Nature Plants, 2021, 7, 1314-1322.	9.3	18
315	Proton and nitrogen electron nuclear double and triple resonance of the chlorophyll a anion in liquid solution. Chemical Physics Letters, 1982, 85, 3-8.	2.6	17
316	25Mg ENDOR and TRIPLE resonance in liquid solution of the bacteriochlorophyll a cation and anion radicals. Chemical Physics Letters, 1984, 111, 583-588.	2.6	17
317	EPR and 55Mn cw-ENDOR study of an antiferrogmagnetically coupled dinuclear manganese (MnIII MnIV) complex. Chemical Physics Letters, 1996, 261, 272-276.	2.6	17
318	Photochemical processes in photosynthesis studied by advanced electron paramagnetic resonance techniques. Pure and Applied Chemistry, 2003, 75, 1021-1030.	1.9	17
319	Incorporation of 2,3-Disubstituted-1,4-Naphthoquinones into the A1 Binding Site of Photosystem I Studied by EPR and ENDOR Spectroscopy. Applied Magnetic Resonance, 2010, 37, 65-83.	1.2	17
320	Ein Redoxhydrogel schützt die O ₂ â€empfindliche [FeFe]â€Hydrogenase aus <i>Chlamydomonas reinhardtii</i> vor oxidativer Zerstörung. Angewandte Chemie, 2015, 127, 12506-12510.	2.0	17
321	Iron-Sulfur Cluster-dependent Catalysis of Chlorophyllide a Oxidoreductase from Roseobacter denitrificans. Journal of Biological Chemistry, 2015, 290, 1141-1154.	3.4	17
322	Bioinspired Artificial [FeFe]-Hydrogenase with a Synthetic H-Cluster. ACS Catalysis, 2019, 9, 4495-4501.	11.2	17
323	EPR in photosynthesis. Electron Paramagnetic Resonance, 0, , 174-242.	0.2	17
324	The radical cation of bacteriochlorophyll b. A liquid-phase endor and triple resonance study. Chemical Physics Letters, 1986, 126, 290-296.	2.6	16

#	Article	IF	CITATIONS
325	EPR and endor studies of cobaloxime(II). Chemical Physics Letters, 1987, 133, 102-108.	2.6	16
326	Bacteriochlorophyll a radical cation and anion—calculation of isotropic hyperfine coupling constants by density functional methods. Physical Chemistry Chemical Physics, 2000, 2, 4772-4778.	2.8	16
327	Photosynthesis: from natural to artificial. Physical Chemistry Chemical Physics, 2014, 16, 11810.	2.8	16
328	Modeling the Active Site of [NiFe] Hydrogenases and the [NiFeu] Subsite of the C-Cluster of Carbon Monoxide Dehydrogenases: Low-Spin Iron(II) Versus High-Spin Iron(II). Inorganic Chemistry, 2014, 53, 6329-6337.	4.0	16
329	Pulse Double-Resonance EPR Techniques for the Study of Metallobiomolecules. Methods in Enzymology, 2015, 563, 211-249.	1.0	16
330	Following [FeFe] Hydrogenase Active Site Intermediates by Time-Resolved Mid-IR Spectroscopy. Journal of Physical Chemistry Letters, 2016, 7, 3290-3293.	4.6	16
331	Local water sensing: water exchange in bacterial photosynthetic reaction centers embedded in a trehalose glass studied using multiresonance EPR. Physical Chemistry Chemical Physics, 2017, 19, 28388-28400.	2.8	16
332	Solvent water interactions within the active site of the membrane type I matrix metalloproteinase. Physical Chemistry Chemical Physics, 2017, 19, 30316-30331.	2.8	16
333	The pheophytin a anion radical. 14N and 1H endor and triple resonance in liquid solution. Chemical Physics Letters, 1982, 90, 375-381.	2.6	15
334	Photo-Induced Electron Spin Polarization in Chemical and Biological Reactions: Probing Structure and Dynamics of Transient Intermediates by Multifrequency EPR Spectroscopy. Applied Magnetic Resonance, 2011, 41, 113-143.	1.2	15
335	Effect of Cyanide Ligands on the Electronic Structure of [FeFe] Hydrogenase Activeâ€6ite Model Complexes with an Azadithiolate Cofactor. Chemistry - A European Journal, 2013, 19, 14566-14572.	3.3	15
336	Spectroscopic Evidence of Reversible Disassembly of the [FeFe] Hydrogenase Active Site. Journal of Physical Chemistry Letters, 2017, 8, 3834-3839.	4.6	15
337	Photoredoxâ€Switchable Resorcin[4]arene Cavitands: Radical Control of Molecular Gripping Machinery via Hydrogen Bonding. Chemistry - A European Journal, 2018, 24, 1431-1440.	3.3	15
338	Carnitine metabolism in the human gut: characterization of the two-component carnitine monooxygenase CntAB from Acinetobacter baumannii. Journal of Biological Chemistry, 2020, 295, 13065-13078.	3.4	15
339	Soft Dynamic Confinement of Membrane Proteins by Dehydrated Trehalose Matrices: High-Field EPR and Fast-Laser Studies. Applied Magnetic Resonance, 2020, 51, 773-850.	1.2	15
340	Molecular Orbital Studies on the Primary Donor P960 in Reaction Centers of Rps. viridis. , 1988, , 379-388.		15
341	B-Branch Electron Transfer in the Photosynthetic Reaction Center of a Rhodobacter sphaeroides Quadruple Mutant. Q- and W-Band Electron Paramagnetic Resonance Studies of Triplet and Radical-Pair Cofactor States. Journal of Physical Chemistry B, 2010, 114, 14364-14372.	2.6	14
342	The structurally unique photosynthetic Chlorella variabilis NC64A hydrogenase does not interact with plant-type ferredoxins. Biochimica Et Biophysica Acta - Bioenergetics, 2017, 1858, 771-778.	1.0	14

#	Article	IF	CITATIONS
343	Nitroxide Spin Labels—Magnetic Parameters and Hydrogen-Bond Formation: A High-Field EPR and EDNMR Study. Applied Magnetic Resonance, 2019, 50, 1-16.	1.2	14
344	13C- and Proton-ENDOR Studies of 13C-labelled Organic Radicals. Zeitschrift Fur Naturforschung - Section A Journal of Physical Sciences, 1978, 33, 514-522.	1.5	14
345	A New Tyrosyl Radical on Phe208 as Ligand to the Diiron Center in Escherichia coli Ribonucleotide Reductase, Mutant R2-Y122H. Journal of Biological Chemistry, 2005, 280, 11233-11246.	3.4	13
346	EPR, ENDOR, and Special TRIPLE measurements of P•+ in wild type and modified reaction centers from Rb.Asphaeroides. Photosynthesis Research, 2009, 99, 1-10.	2.9	13
347	Intersubunit distances in full-length, dimeric, bacterial phytochrome Agp1, as measured by pulsed electron-electron double resonance (PELDOR) between different spin label positions, remain unchanged upon photoconversion. Journal of Biological Chemistry, 2017, 292, 7598-7606.	3.4	13
348	Spectroscopic investigations of a semi-synthetic [FeFe] hydrogenase with propane di-selenol as bridging ligand in the binuclear subsite: comparison to the wild type and propane di-thiol variants. Journal of Biological Inorganic Chemistry, 2018, 23, 481-491.	2.6	13
349	15N Endor Experiments on the Primary Donor Cation Radical D+ in Bacterial Reaction Center Single Crystals of RB. Shaeroides R-26. , 1992, , 89-97.		13
350	Esr and endor studies of partially deuterated and chlorinated phenalenyls. Tetrahedron, 1978, 34, 419-424.	1.9	12
351	Covalent Attachment of the Waterâ€insoluble Ni(P Cy 2 N Phe 2) 2 Electrocatalyst to Electrodes Showing Reversible Catalysis in Aqueous Solution. Electroanalysis, 2016, 28, 2452-2458.	2.9	12
352	Paramagnetic Molecular Grippers: The Elements of Six-State Redox Switches. Journal of Physical Chemistry Letters, 2016, 7, 2470-2477.	4.6	12
353	Möbius–Hückel Topology Switching in Expanded Porphyrins: EPR, ENDOR, and DFT Studies of Doublet and Triplet Open-Shell Systems. Applied Magnetic Resonance, 2016, 47, 757-780.	1.2	12
354	Structured near-infrared Magnetic Circular Dichroism spectra of the Mn4CaO5 cluster of PSII in T. vulcanus are dominated by Mn(IV) d-d â€̃spin-flip' transitions. Biochimica Et Biophysica Acta - Bioenergetics, 2018, 1859, 88-98.	1.0	12
355	Thermally Activated Delayed Fluorescence in a Y ₃ N@C ₈₀ Endohedral Fullerene: Timeâ€Resolved Luminescence and EPR Studies. Angewandte Chemie - International Edition, 2018, 57, 277-281.	13.8	12
356	Investigation of Rhodobacter Sphaeroides Reaction Center Mutants with Changed Ligands to the Primary Donor. , 1998, , 767-770.		12
357	13C- and 1H-ENDOR Studies of a Phenoxyl Type Radical. Zeitschrift Fur Naturforschung - Section A Journal of Physical Sciences, 1978, 33, 1072-1076.	1.5	11
358	Crystallization and preliminary X-ray crystallographic analysis of the catalytic domain of membrane type 1 matrix metalloproteinase. Acta Crystallographica Section F, Structural Biology Communications, 2014, 70, 232-235.	0.8	10
359	Elucidation of the heme active site electronic structure affecting the unprecedented nitrite dismutase activity of the ferriheme b proteins, the nitrophorins. Chemical Science, 2016, 7, 5332-5340.	7.4	10
360	Polymer-Bound DuBois-Type Molecular H ₂ Oxidation Ni Catalysts Are Protected by Redox Polymer Matrices. ACS Applied Energy Materials, 2019, 2, 2921-2929.	5.1	10

#	Article	IF	CITATIONS
361	In Vivo Biogenesis of a De Novo Designed Iron–Sulfur Protein. ACS Synthetic Biology, 2020, 9, 3400-3407.	3.8	10
362	EPR Studies of the Primary Electron Donor P700 in Photosystem. , 2006, , 245-269.		10
363	Magnetic Resonance and Molecular Orbital Studies of the Primary Donor States in Bacterial Reaction Centers. Jerusalem Symposia on Quantum Chemistry and Biochemistry, 1990, , 423-434.	0.2	10
364	Study of heme Fe(III) ligated by OH-in cytochromeb-559 and its low temperature photochemistry in intact chloroplasts. FEBS Letters, 1995, 377, 325-329.	2.8	9
365	A New Stable High-Valent Diiron Center in R2 Mutant Y122H ofE.coliRibonucleotide Reductase Studied by High-Field EPR and57Fe-ENDOR. Journal of the American Chemical Society, 2000, 122, 9856-9857.	13.7	9
366	Pulse Q-Band EPR and ENDOR Spectroscopies of the Photochemically Generated Monoprotonated Benzosemiquinone Radical in Frozen Alcoholic Solution. Journal of Physical Chemistry B, 2012, 116, 8890-8900.	2.6	9
367	A caged substrate peptide for matrix metalloproteinases. Photochemical and Photobiological Sciences, 2015, 14, 300-307.	2.9	9
368	1H NMR Spectroscopy of [FeFe] Hydrogenase: Insight into the Electronic Structure of the Active Site. Journal of the American Chemical Society, 2018, 140, 131-134.	13.7	9
369	Viologen-modified electrodes for protection of hydrogenases from high potential inactivation while performing H ₂ oxidation at low overpotential. Dalton Transactions, 2018, 47, 10685-10691.	3.3	9
370	Spin-dependent recombination of the charge-transfer state in photovoltaic polymer/fullerene blends. Molecular Physics, 2019, 117, 2654-2663.	1.7	9
371	Primary donor triplet states of Photosystem I and II studied by Q-band pulse ENDOR spectroscopy. Photosynthesis Research, 2022, , 1.	2.9	9
372	The Magic of Disaccharide Glass Matrices for Protein Function as Decoded by High-Field EPR and FTIR Spectroscopy. Applied Magnetic Resonance, 2015, 46, 435-464.	1.2	8
373	The Laser-Induced Potential Jump: A Method for Rapid Electron Injection into Oxidoreductase Enzymes. Journal of Physical Chemistry B, 2020, 124, 8750-8760.	2.6	8
374	Spin Polarization Reveals the Coordination Geometry of the [FeFe] Hydrogenase Active Site in Its CO-Inhibited State. Journal of Physical Chemistry Letters, 2020, 11, 4597-4602.	4.6	7
375	Metallofullerene photoswitches driven by photoinduced fullerene-to-metal electron transfer. Chemical Science, 2021, 12, 7818-7838.	7.4	7
376	Radical Products in Single Electron Transfer Reactions of Lithium Triethylhydridoborate as Detected by ESR and Multinuclear (1H,10B,11B,14N) ENDOR Spectroscopy. Angewandte Chemie International Edition in English, 1983, 22, 1209-1220.	4.4	6
377	Comparative ENDOR study at 34ÂGHz of the triplet state of the primary donor in bacterial reaction centers of Rb. sphaeroides and Bl. viridis. Photosynthesis Research, 2014, 120, 99-111.	2.9	6
378	A [RuRu] Analogue of an [FeFe]â€Hydrogenase Traps the Key Hydride Intermediate of the Catalytic Cycle. Angewandte Chemie, 2018, 130, 5527-5530.	2.0	6

#	Article	IF	CITATIONS
379	An improved coupling design for high-frequency TE011 electron paramagnetic resonance cavities. Review of Scientific Instruments, 2013, 84, 014704.	1.3	5
380	Protein Crystallography Using Freeâ€Electron Lasers: Water Oxidation in Photosynthesis. Angewandte Chemie - International Edition, 2014, 53, 13007-13008.	13.8	5
381	Synthesis and Characterization of Nickel Compounds with Tetradentate Thiolate–Thioether Ligands as Precursors for [NiFe]–Hydrogenase Models. European Journal of Inorganic Chemistry, 2014, 2014, 148-155.	2.0	5
382	Vibrational Perturbation of the [FeFe] Hydrogenase H-Cluster Revealed by ¹³ C ² H-ADT Labeling. Journal of the American Chemical Society, 2021, 143, 8237-8243.	13.7	4
383	Hydrogen-Bonded Complexes of Neutral Nitroxide Radicals with 2-Propanol Studied by Multifrequency EPR/ENDOR. Applied Magnetic Resonance, 0, , 1.	1.2	4
384	Molecular Concepts of Water Splitting: Nature's Approach. Green, 2013, 3, .	0.4	2
385	Thermally Activated Delayed Fluorescence in a Y ₃ N@C ₈₀ Endohedral Fullerene: Timeâ€Resolved Luminescence and EPR Studies. Angewandte Chemie, 2018, 130, 283-287.	2.0	2
386	Bioenergetics Theory and Components Hydrogenases Structure and Function. , 2021, , 66-73.		2
387	Eine Redoxpolymerâ€basierte Gasdiffusionsâ€H 2 â€Oxidationsbioanode mit hoher Stromdichte unter Verwendung von [FeFe]â€Hydrogenase aus Desulfovibrio desulfuricans integriert in einer membranfreien Biobrennstoffzelle. Angewandte Chemie, 2020, 132, 16649.	2.0	2
388	Time-Resolved Infrared Spectroscopy Reveals the pH-Independence of the First Electron Transfer Step in the [FeFe] Hydrogenase Catalytic Cycle. Journal of Physical Chemistry Letters, 0, , 5986-5990.	4.6	2
389	Probing the Electronic Structure of Bacteriochlorophyll Radical Ions—A Theoretical Study of the Effect of Substituents on Hyperfine Parameters. Photochemistry and Photobiology, 2017, 93, 755-761.	2.5	1
390	Remembering George Feher (1924–2017). Photosynthesis Research, 2018, 137, 361-375.	2.9	1
391	Enhancing the catalytic current response of H 2 oxidation gas diffusion bioelectrodes using an optimized viologenâ€based redox polymer and [NiFe] hydrogenase. Electrochemical Science Advances, 0, , e2100100.	2.8	1
392	Jim Hyde and the ENDOR Connection: A Personal Account. Applied Magnetic Resonance, 2017, 48, 1149-1183.	1.2	0
393	Special Issue of Applied Magnetic Resonance Celebrating the 85th Birthdays of Klaus Möbius and Kev M. Salikhov. Applied Magnetic Resonance, 2022, 53, 457.	1.2	0
394	CIDEP-Enhanced ENDOR of short-lived radicals. Recollections of first joint experiments with Renad Sagdeev. Russian Chemical Bulletin, 2021, 70, 2445-2456.	1.5	0